ELSEVIER

International Journal of Heat and Fluid Flow 23 (2002) 340–345

International Journal of HEAT AND FLUID FLOW

www.elsevier.com/locate/ijhff

Conjugate heat transfer predictions in two-dimensional ribbed passages ☆

G. Iaccarino [a,*], A. Ooi [b], P.A. Durbin [c], M. Behnia [d]

[a] *Center for Turbulence Research, Stanford University, Stanford, CA 94305-3030, USA*
[b] *Department of Mechanical and Manufacturing Engineering, University of Melbourne, Melbourne 3010, Australia*
[c] *Department of Mechanical Engineering, Stanford University, Stanford, CA 94305-3030, USA*
[d] *School of Mechanical and Manufacturing Engineering, University of New South Wales, Sydney 2052, Australia*

Abstract

The effect of thermal boundary conditions on numerical heat transfer predictions in rib-roughened passages is investigated. Results obtained using constant heat flux at the walls and conjugate heat transfer are compared to illustrate how the recirculation bubbles upstream and downstream of the rib have different effects on the local heat transfer. Comparison between numerical predictions, experimental measurements and data correlations show that the predicted heat transfer is very sensitive to the type of boundary conditions used in the numerical model. It is illustrated that some of the discrepancies observed between experimental and numerical data can be eliminated if conduction heat transfer in the rib is taken into account. © 2002 Published by Elsevier Science Inc.

1. Introduction

Nowadays, sophisticated numerical techniques based on the solution of the Reynolds-averaged Navier–Stokes (RANS) equations are being used to predict heat transfer in complex passages (Simoneau and Simon, 1992). One of the factors determining the accuracy of RANS heat transfer predictions is the turbulence model used in the predictions. Numerical studies conducted by Ooi et al. (submitted for publication), Iacovides and Raisee (1999), Stephens (1995) and Liou et al. (1993) have evaluated the accuracy of some of the more commonly used turbulence models by comparing numerical predictions with the experimental data of Bredberg and Davidson (1999), Rau et al. (1998), Liou et al. (1993), Chyu and Wu (1989), Han et al. (1985) and Han et al. (1978). The numerical studies concluded that accuratenear-wall modeling of turbulence transport is crucialto ensure good predictions (Iacovides and Raisee, 1999).

Another key factor that determines the accuracy of the heat transfer prediction is the thermal boundary condition that is used at the walls of the ribs. In all numerical studies that have been carried out thus far, constant heat flux is employed as a boundary condition on the rib walls. The effects of conduction heat transfer in the walls have not been considered. In real passages, the heat transfer process that occur is always a combination of forced convection and heat conduction. Therefore, it might be more appropriate to assess the accuracy of the numerical model by performing conjugate heat transfer calculations whereby both the convection and conduction heat transfer are calculated as part of the solution. This is suggested in the experimental data cited above as, depending on the technique used and on the materials and the experimental set-up, very different values of heat transfer are measured. For example, the experimental data in Fig. 5 show a large variation in the measured values of the Nusselt number, Nu between Reynolds number, $Re = 100\,000$ and $122\,000$ which cannot be explained by the modest differences in Re alone. In this study, it will be shown that the differences in the local values of Nu can be attributed to the different experimental set-ups.

☆ This paper is a revised and expanded version of a paper presented at CHT'01, the Second International Symposium on Advances in Computational Heat Transfer (Palm Cove, Qld., Australia, 20–25 May 2001), the proceedings of which were published by Begell House, Inc.

* Corresponding author. Tel.: +1-650-723-9599; fax: +1-650-723-0617.

E-mail address: jops@ctr.stanford.edu (G. Iaccarino).

0142-727X/02/$ - see front matter © 2002 Published by Elsevier Science Inc.
PII: S0142-727X(02)00181-9

In the present work, the $\overline{v'^2}$–f and two k–ϵ turbulence models are used to predict the flow and the heat transfer in two-dimensional ribbed passages. The predicted averaged heat transfer is compared with experimental correlations to illustrate that the average heat transfer is related to the large scale flow field motion (separation lengths, etc.). The turbulence models determine the size of the separation bubble and hence directly determine the predicted average heat transfer. For the conjugate heat transfer predictions, only the $\overline{v'^2}$–f turbulence model is considered, as the main focus will be on how the predicted heat transfer data is influenced by the rib wall thermal conditions.

2. Numerical model

In all the cases considered in this paper, the geometry is periodic in the streamwise direction. Hence, as shown in Fig. 1(a), only one section of the actual ribbed passage will be considered. The mean velocity field is assumed to be fully developed which will allow the use of periodic boundary conditions in the streamwise direction. The temperature and pressure fields contain a non-periodic contribution, but it is a constant gradient. These two quantities can be decomposed into a periodic part plus a linear varying term (in the periodic direction). The governing equations are modified to account for this additional term and the equations of motion can be solved to obtain a fully periodic solution. Unstructured grids are used to allow for normal-to-the-wall clustering on both sides of the passage, with different resolution in the streamwise direction (Fig. 1(b)).

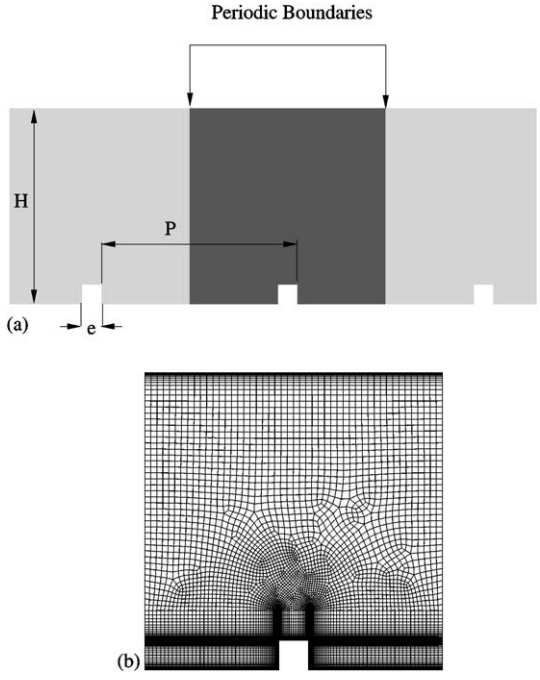

Fig. 1. Computational domain (a) and mesh (b) for the periodic flow in a ribbed channel or pipe.

The two-dimensional incompressible RANS equations are solved. Turbulent fluctuations are accounted for using the Boussinesq eddy-viscosity assumption. The energy equation is solved in the following form:

$$\frac{\partial E}{\partial t}+\frac{\partial}{\partial x_i}(u_i(E+p/\rho))=\frac{\partial}{\partial x_i}\left[(k_{\mathrm{f}}+k_{\mathrm{t}})\frac{\partial T}{\partial x_i}\right], \tag{2.1}$$

where E is the total energy, k_{f} is the thermal conductivity and k_{t} is the thermal eddy diffusivity. The Prandtl ($Pr=\nu/k_{\mathrm{f}}$) number is set to a constant value of 0.7. The viscous heating is negligible and a constant turbulent Prandtl number ($Pr_{\mathrm{t}}=0.9$) is introduced to model the turbulent heat flux,

$$k_{\mathrm{t}}=\nu_{\mathrm{t}}/Pr_{\mathrm{t}}, \tag{2.2}$$

where ν_{t} is the eddy viscosity obtained from the turbulence model. Most of the results in this paper are predicted using the $\overline{v'^2}$–f turbulence model (Durbin, 1995). However, for reference, the predictive capability of the turbulence models proposed by Rodi (1991) and Launder and Sharma (1974) will also be considered. The equations governing the turbulence models will not be give here. Readers who are interested in the models are advised to consult the papers above.

Different variations of thermal boundary condition on the ribs are considered in this study. These simulations are meant to assess the effect of uncertainty in the experimental conditions (which can be due to the measurement technique, the rib and channel wall material properties, the presence of unsteady effects, etc.) on the predicted data. Constant heat flux is simulated by specifying the temperature gradients at all walls (see Fig. 2(c)). This is opposite to the real operative condition, where the fluid is hot and heat is removed by the passage walls. For conjugate heat transfer calculations (see Fig. 2(b)), both the conduction and convection heat transfer is simulated and the equations are coupled at the walls. On the fluid side, u_i in Eq. (2.1) is the local fluid velocity. However, on the solid side (i.e. inside the walls) u_i in Eq. (2.1) is set to zero and the thermal conductivity is set to k_{s}. The last case considered in this paper is where the rib is insulated (Fig. 2(a)). For this case, the temperature gradient normal to the rib walls is set to zero.

A commercial CFD code, FLUENT, has been used in this work. The code solves the incompressible RANS equations using a second order upwind scheme and the SIMPLE pressure–velocity coupling technique. The additional equations for the turbulent quantities are solved afterward in a segregated fashion. The $\overline{v'^2}$–f model has been implemented by the authors (see Iaccarino (2001) for details); all the other turbulence models are available directly in FLUENT.

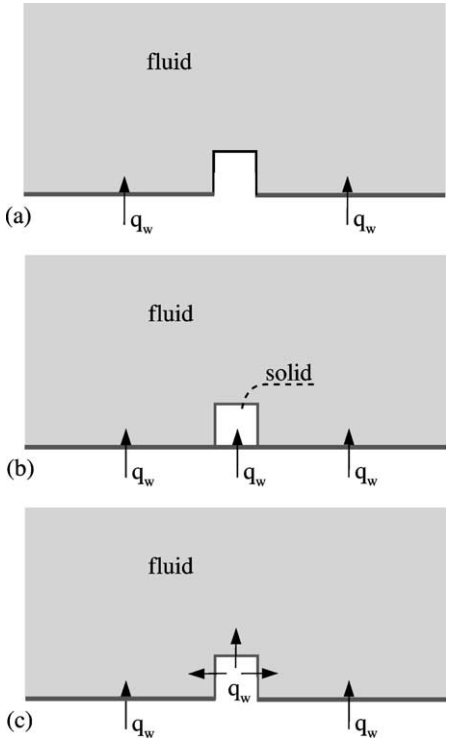

Fig. 2. Wall thermal conditions: (a) rib insulated, (b) solid–fluid simulation, constant heat flux at the base of the rib and (c) constant heat flux at the rib surface.

3. Results and discussion

3.1. Averaged heat transfer predictions

Axi-symmetric flow simulations were carried out for a range of Reynolds numbers, Re with P/D ranging from 1 to 3 and with various values of roughness parameter e/D. The predicted averaged Nusselt number is shown in Fig. 3. The data are obtained at $Re = 12\,600$, $e/D = 0.1$ and $P/D = 1$ and varying one parameter for each of Fig. 3(a)–(c) while leaving the other parameters unchanged. The data in this figure are normalized with the corresponding value of Nusselt number for smooth tubes

$$Nu_s = 0.02\,Re^{0.8}. \tag{3.1}$$

The numerical results are compared with the correlation presented in Ravigururajan and Bergles (1996),

$$Nu/Nu_s = \left(1 + \left[2.617\,Re^{0.036}(e/D)^{0.212}(P/D) - 0.21\right]^7\right)^{1/7} \tag{3.2}$$

in order to assess the accuracy of the predictions.

Results obtained using the $\overline{v'^2}$–f model are consistently closer to the experimental correlation than those obtained using the other two k–ϵ models. The model of Launder and Sharma (1974) overestimates and the model of Rodi (1991) underestimates the heat flux. Simulations were also carried out using the $\overline{v'^2}$–f model but with zero heat flux boundary conditions at the ribs, to assess the effect of changing the thermal boundary condition on the predictions. It is clear looking at the data in Fig. 3(a)–(c) that the difference between near-wall treatments in the turbulence model is much larger than the difference between the various thermal boundary conditions.

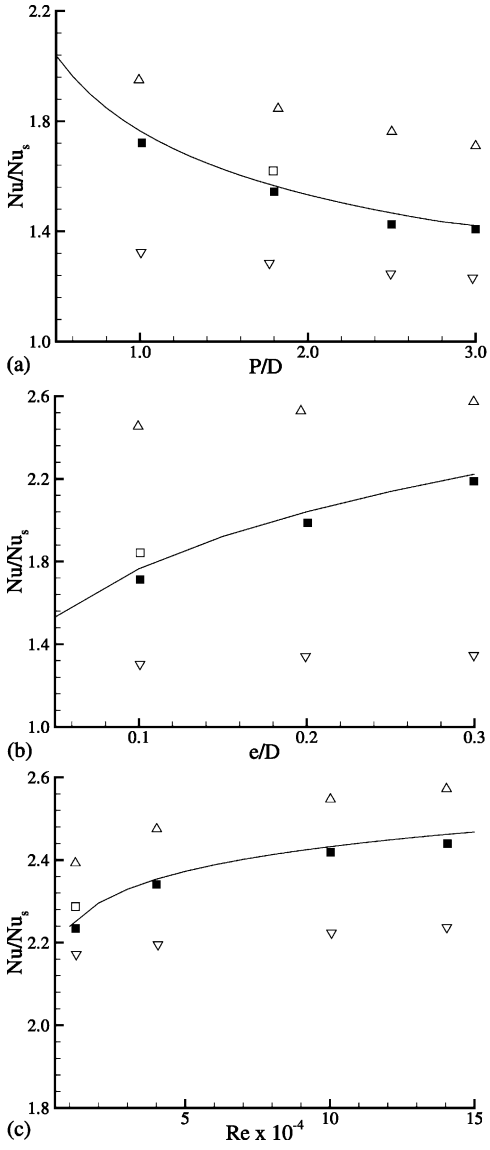

Fig. 3. Averaged heat transfer enhancement in pipes: (a) effect of the pitch, P/D; (b) effect of the roughness e/D; (c) effect of the Reynolds number, Re. (—) Correlation of experimental data (Ravigururajan and Bergles, 1996), (■) $\overline{v'^2}$–f with heated rib, (□) $\overline{v'^2}$–f with insulated rib, (△) k–ε (Launder and Sharma, 1974), (▽) k–ε (Rodi, 1991).

The difference in the averaged heat transfer predictions is related to the large scale motion of the flow field (separation lengths, etc.). This is can be seen from the flow patterns computed at $Re = 40\,000$ using different turbulent models, shown in Fig. 4. It can be seen that

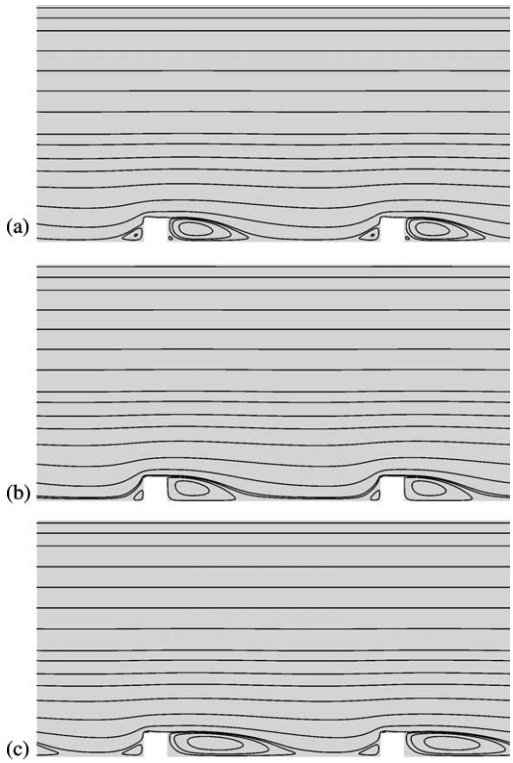

Fig. 4. Streamlines in a rib-roughened pipe at $Re = 40\,000$; (a) k–ε (Launder and Sharma, 1974), (b) k–ε (Rodi, 1991), (c) $\overline{v'^2}$–f.

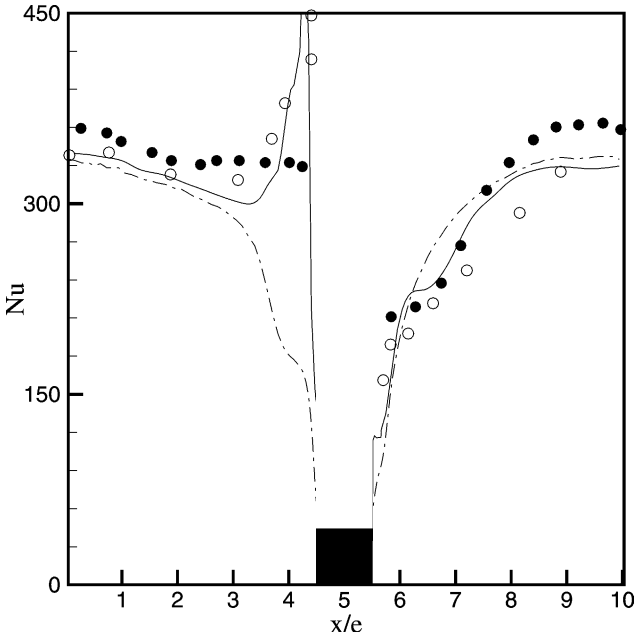

Fig. 5. Nusselt number on the floor of the channel. Experiments: (○) $Re = 100\,000$, (●) $Re = 122\,000$; simulations ($Re = 100\,000$, $\overline{v'^2}$–f): (– - –) heated rib, (—) insulated rib.

both k–ϵ models predict a small recirculation bubble downstream of the rib. The results obtained with the $\overline{v'^2}$–f model show a larger extent of separation. Lower turbulence levels in the recirculation bubble account for the lower value of predicted Nu using the $\overline{v'^2}$–f model as compared to the k–ϵ models.

3.2. Local heat transfer predictions: effects of thermal boundary conditions

The local Nu distribution obtained experimentally at $Re = 100\,000$ and $122\,000$ is shown in Fig. 5. Also shown in this figure are numerical predictions obtained using the $\overline{v'^2}$–f turbulence model. The overall agreement is satisfactory in terms of the heat transfer level attained away from the rib. However, the two sets of experimental data show large differences upstream of the rib that cannot be justified solely by the modest increase in the Reynolds number. This can be due to uncertainties in the measurements (different techniques were used) or differences in the experimental set-up. Another possible explanation would be how the ribs are "treated". This is clear from the numerical data obtained using the $\overline{v'^2}$–f model at $Re = 100\,000$ but with different thermal boundary condition for the rib. When the rib is heated, the predicted value of Nu is very close to zero, directly upstream of the rib. When the rib is insulated, the model predicts large values of Nu in that region.

In order to obtain a better understanding on how heat is transferred from the ribs, conjugate heat transfer calculations were carried out. These additional computations show that the predicted heat transfer is very sensitive to the type of thermal boundary conditions used in the simulations. The recirculation regions upstream and downstream of the rib have opposite effects on the conjugate heat transfer. In the *upstream* bubble, cold flow impinges on the rib side wall and then moves towards the floor of the channel. If the rib material has high conductivity this fluid is heated before it reaches the floor. If the rib has low conductivity, the impinging flow cools the lower wall at the base of the rib. In the *downstream* bubble, the flow is reversed and heated fluid is convected toward the rib side wall, then up and away from the floor.

The thermal field is uncoupled from the velocity field and therefore only the temperature distributions must be analyzed. In Fig. 6 temperature contours in the vicinity of the rib are reported. The dark area in the figure corresponds to lower temperatures—and, thus, to higher Nusselt numbers on the surface. The conjugate heat transfer calculation of Fig. 6(b) is for the same conductivity of the fluid and the solid ($k_f = k_s$). The qualitative and quantitative features of the solution corresponding to the solid–fluid coupled thermal field (Fig. 6(b)) are in between the adiabatic (Fig. 6(c)) and prescribed heat flux (Fig. 6(a)) cases.

Data in Fig. 6 show that the region downstream of the rib is not dramatically affected by the various thermal boundary conditions. On the other hand, the area

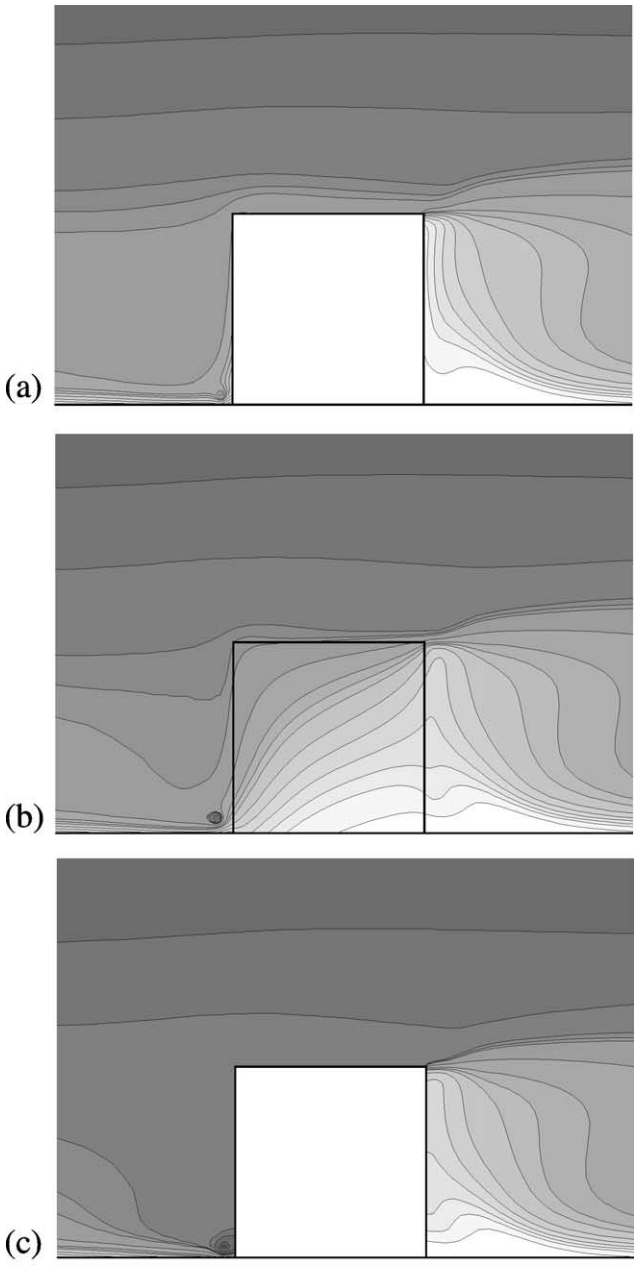

Fig. 6. Temperature distribution in the vicinity of the rib. Effect of the wall thermal condition: (a) heated rib, (b) solid–fluid coupling and (c) insulated rib. Predictions obtained using the $\overline{v'^2}$–f model. $Re = 10\,000$.

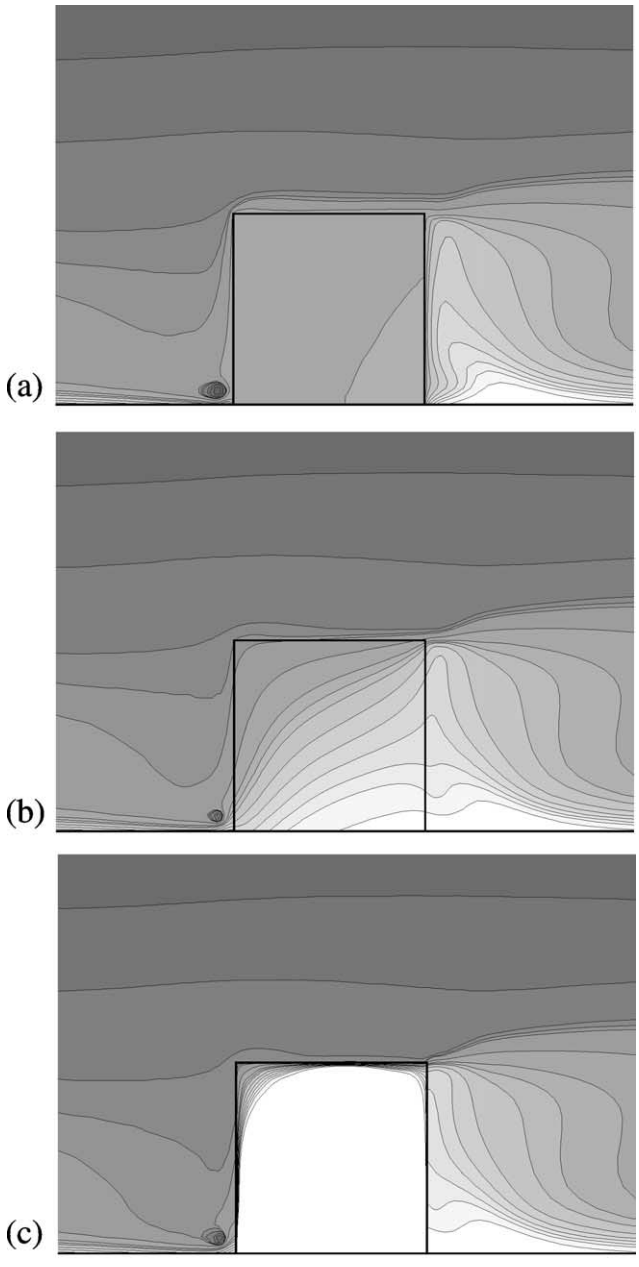

Fig. 7. Temperature distribution in the vicinity of the rib. Effect of the rib thermal conductivity: (a) $k_s/k_f = 100$, (b) $k_s/k_f = 1$ and (c) $k_s/k_f = 0.01$. Predictions obtained using the $\overline{v'^2}$–f model. $Re = 10\,000$.

upstream of the rib shows large differences: when the rib side wall is heated, the fluid that impinges in the channel floor is approximately at the same temperature as the wall. When the side rib wall is adiabatic (see Fig. 6(c)), cold fluid reaches the floor and correspondingly high levels of Nu are predicted.

The effect of varying the rib thermal conductivity (k_s) is investigated in Fig. 7. Temperature fields corresponding to high and low conductivity are reported in the figure. The upstream region does not show a strong dependency on k_s because the heat transfer is dominated by convection. The downstream region, on the other hand, is dramatically changed because, near the rib, heat is removed from the fluid mainly by conduction. This is further illustrated by the surface Nusselt number (Fig. 8). The two limiting conditions of insulated and heated ribs show nearly the same levels of heat transfer in the downstream region. Upstream, as noted previously, cold fluid reaches the floor when the rib side wall is not heated. The analysis of the conjugate heat transfer predictions shows that conduction plays a major role in the downstream area. Results at other Reynolds numbers are consistent with this observation.

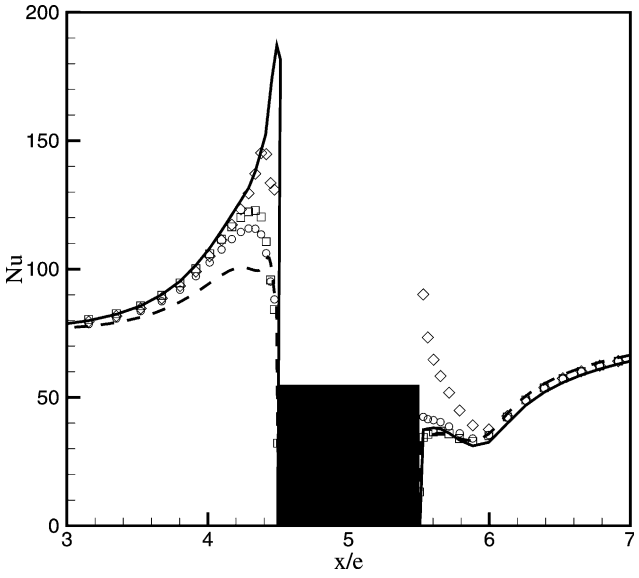

Fig. 8. Nusselt number on the floor of the channel. Effect of the wall thermal condition and the rib conductivity. (—) Insulated rib, (– – –) heated rib, (◇) $k_s/k_f = 100$, (○) $k_s/k_f = 1$ and (□) $k_s/k_f = 0.01$. Predictions obtained using the $\overline{v'^2}$–f model.

The level of the heat transfer away from the rib is only slightly altered by the rib boundary condition. This gives confidence in the good agreement with the measurements presented in the previous sections. On the other hand, the differences in the vicinity of the ribs are substantial. Hence, differences observed between the experimental data in Fig. 5 could be related to differences between the experimental set-ups. Fig. 8 illustrates that clearly prescribed surface conditions are needed in order to accurately test numerical predictions on the wall adjacent to the rib.

4. Concluding remarks

RANS simulations are used routinely in industry for design purposes. In this work, a detailed analysis of the capabilities of the $\overline{v'^2}$–f turbulence model for predicting the heat transfer in rib-enhanced passages is presented. The $\overline{v'^2}$–f is compared to other *classical* turbulence closures to establish its merits; several configurations and flow conditions are examined to assess its value as a design tool. The results are satisfactory and show that the model consistently reproduces the correct levels of heat transfer.

A study on the effect of the thermal wall boundary condition on the prediction of heat transfer. It is shown that predicted *averaged* values of the Nusselt number closely matches the experimental data. However, the *local* values of Nusselt number very close to the ribs are strongly affected by the wall thermal boundary condition on the rib. The numerical data show that the heat transfer is dominated by convection upstream and conduction downstream of the rib.

References

Bredberg, J., Davidson, L., 1999. Prediction of flow and heat transfer in a stationary 2D rib-roughened passage using low-Re turbulent models. In: 3rd European Conference on Turbomachinery, pp. 963–972.

Chyu, M.K., Wu, L.X., 1989. Combined effects of rib angle-of-attack and pitch-to-height ratio on mass transfer from a surface with transverse ribs. Exp. Heat Transfer 2, 291–308.

Durbin, P.A., 1995. Separated flow computations with the v^2–f model. AIAA J. 33, 659–664.

Han, J.C., Glicksman, L.R., Rohsenow, W.M., 1978. An investigation of heat transfer and friction for rib-roughened surfaces. Int. J. Heat Mass Transfer 21, 1143–1156.

Han, J.C., Park, J.S., Lei, C.K., 1985. Heat transfer enhancement in channels with turbulence promoters. J. Eng. Gas Turbines Power 107, 628–635.

Iacovides, H., Raisee, M., 1999. Recent progress in the computation of flow and heat transfer in internal cooling passages of turbine blades. Int. J. Heat Fluid Flow 20, 320–328.

Iaccarino, G., 2001. Prediction of a turbulent separated flow using commercial CFD codes. ASME J. Fluids Eng. 123 (4), 1–9.

Launder, B.E., Sharma, A., 1974. Application of the energy-dissipation model of turbulence to the calculation of flow near a spinning disk. Lett. Heat Mass Transfer 1, 131–138.

Liou, T.M., Hwang, J.J., Chen, S.H., 1993. Simulation and measurement of enhanced turbulent heat transfer in a channel with periodic ribs on one principal wall. Int. J. Heat Mass Transfer 36 (2), 507–517.

Ooi, A., Iaccarino, G., Durbin, P.A., Behnia, M. Reynolds averaged simulation of flow and heat transfer in ribbed ducts. Int. J. Heat Fluid Flow, submitted for publication.

Rau, G., Cakan, M., Moeller, D., Arts, T., 1998. The effect of periodic ribs on the local aerodynamic and heat transfer performance of a straight cooling channel. J. Turbomachinery 120, 368–375.

Ravigururajan, T.S., Bergles, A.E., 1996. Development and verification of general correlations for pressure drop and heat transfer in single-phase turbulent flow in enhanced tubes. Exp. Thermal Fluid Sci. 13 (1), 55–71.

Rodi, W., 1991. Experience with two-layer models combining the k–ϵ model with a one-equation model near the wall. AIAA Paper 91-0216.

Simoneau, R.J., Simon, F.F., 1992. Progress towards understanding and predicting heat transfer in the turbine gas path. Int. J. Heat Fluid Flow 14 (2), 106–128.

Stephens, M.A., 1995. Computation of flow and heat transfer in a rectangular channel with ribs. AIAA Paper 95-0180 117 (3), 417–423.